

Potential models for ionic oxides

To cite this article: G V Lewis and C R A Catlow 1985 *J. Phys. C: Solid State Phys.* **18** 1149

View the [article online](#) for updates and enhancements.

Related content

- [Defect properties of ionic solids. II. Point defect energies based on modified electron-gas potentials](#)
- [Defect properties of ionic solids. III. The calculation of the point-defect structure of the alkaline-earth oxides and CdO](#)
- [Ionicity in solids](#)

Recent citations

- [Defect structure and vibrational states in Eu-doped cubic gadolinium oxide](#)
Alexey N. Kislov and Anatoly F. Zatsepin
- [Intrinsic defects and non-stoichiometry in undoped cadmium silicate hosts](#)
Eduily Benvindo Vaz Freire *et al*
- [The interaction of nanoparticulate Fe₃O₄ during the diffusion-limited aggregation process: A molecular dynamics simulation](#)
ZhengJian Liu *et al*

Potential models for ionic oxides

G V Lewis and C R A Catlow

Department of Chemistry, University College London, 20 Gordon Street, London WC1H 0AJ, UK

Received 29 June 1984

Abstract. We present a systematic approach to the derivation of empirical potential parameters for binary oxides; we also consider their modification for use in mixed oxide systems. Shell-model potentials are used but, unlike the case for the alkali halides within which polarisability and short-range interaction parameters can be transferred, modifications must be introduced when transferring potential parameters between different oxides. The anion polarisability varies with structure and with the nature of the host cation, and changes in cation coordination are reflected in the short-range repulsive cation–anion interaction. Parameters are derived for a range of oxides, and trends in these parameters are discussed. We discuss successful applications of the potentials to the calculation of perfect lattice properties. Equal success is enjoyed when defect and surface properties are considered; in particular our models correctly predict the activation energies for dopant diffusion in NiO, and to a large extent model the surface rumpling of MgO.

1. Introduction

There have been several studies in recent years of interatomic potentials for ionic and semi-ionic solids (see e.g. Catlow *et al* 1982, Catlow and Stoneham 1983 for recent reviews). This work is stimulated in part by the importance of potential models in understanding cohesive, elastic and lattice dynamical properties of these solids. Interatomic potentials are also the key factor in determining the reliability of computer modelling studies which have been widely applied to perfect lattice and defect properties of ionic materials (Mackrodt 1984, Catlow and Mackrodt 1982).

To date, most potentials for oxides and halides have been based on the assumption of the fully ionic model (see Catlow and Stoneham (1983) for a discussion of this assumption), with ionic polarisability treated by the shell model of Dick and Overhauser (1958), and with central-force, pairwise short-range potentials described usually by a simple analytical function, most commonly the Born–Mayer potential supplemented by an attractive, r^{-6} term, i.e.

$$V_{ij}(r_{ij}) = A_{ij} \exp(-r_{ij}/\rho) - C_{ij}r_{ij}^{-6}. \quad (1)$$

Potential parameters (A , ρ , and C in the above equation and the shell charges, Y and spring constant, K , associated with the shell-model description of polarisability) have most commonly been derived by the procedure of ‘empirical fitting’, i.e. parameters are adjusted, usually by a least-squares fitting routine, so as to achieve the best possible agreement between calculated and experimental crystal properties.

If the latter procedure is to be carried out successfully, a wide range of crystal properties should be used, including structural, elastic, dielectric, and lattice dynamical data. For many oxides, however, only the structure and lattice constant are known. There is therefore insufficient data to determine all the unknown parameters in the shell model potentials of these materials. In addition, whereas potential parameters can be chosen to be transferable for the alkali halides a similar approach for oxides is unsuccessful, since the oxide ion does not exist as a stable free ion, the second electron being bound only by the Madelung potential. Hence we may expect a strong variation in electronic polarisability with crystalline environment for ionic oxides. This is indeed apparent from the work of Sangster and Stoneham (1980) who derived a systematic set of potentials for the rocksalt structured oxides. Polarisability values were constrained by the expression

$$\alpha_+ + \alpha_- = \alpha + \beta_0^{-1}(z - z')^2 \quad (2)$$

where

$$\alpha = \frac{3V_c \epsilon_0 - 1}{4\pi \epsilon_0 + 2} \quad (3)$$

and

$$\beta_0^{-1} = \frac{M\omega_0^2 \epsilon_0 + 2}{e^2 \epsilon_\infty + 2} \quad (4)$$

in which ϵ_0 , ϵ_∞ are the static and high-frequency dielectric constants, ω_0 is the TO frequency, M is the reduced mass, Z is the ionic charge and Z' is the Szegedi charge. By assuming the oxygen polarisability is constant and the polarisability of Mg^{2+} is negligible, the cation polarisabilities are found to be unreasonably large, although a similar scheme has proved successful for the alkali halides (Catlow *et al* 1979). Sangster and Stoneham (1980) concluded that either the oxygen polarisability is strongly dependent upon crystal environment or some other mechanism is operating or that a combination of both factors is responsible.

Further evidence for the non-transferability of shell parameters in oxides was found by Mahan (1980) who has calculated ionic polarisabilities for a series of rocksalt oxides and found a significant variation in anion polarisability with crystalline environment whereas cation polarisabilities show no significant changes. In particular the polarisability of negative ions is found to depend inversely upon the lattice constant.

The first aim of this paper is to indicate how these problems which are inherent in the modelling of binary oxides, unlike the alkali halides, can be incorporated into a shell-model description in a simple but effective manner. We also consider a further problem which concerns the extent to which short-range potential parameters derived for binary oxides may be used in the study of ternary oxide crystals. For example, if we derive potential parameters representing short-range interactions between Mg^{2+} ions and O^{2-} ions in MgO and Al^{3+} and O^{2-} in Al_2O_3 can the same parameters be used in a realistic stimulation of MgAl_2O_4 ? How is the interaction affected by the coordination of the cation which for Mg^{2+} changes from octahedral in MgO to tetrahedral in MgAl_2O_4 ?

In the present paper, therefore, we propose a systematic approach to the empirical parameters of potential models for ternary oxides which takes account of (i) the paucity of experimental data for some oxides, (ii) the crystal dependence of oxygen polarisability, and (iii) the coordination dependence of short-range potentials. We show that

our potentials succeed in a variety of applications, and we consider the physical significance of the trends in the potential parameters that we derive.

2. Derivation of potential parameters for oxides

2.1. Modelling of anion polarisability

For the shell model the value of the free-ion electronic polarisability is given by the expression:

$$\alpha = Y^2/k \quad (5)$$

where Y is the shell charge and k the harmonic spring constant coupling the shell and core of the ion. For isostructural oxides, as argued by Mahan (1980) we may assume that there is an approximately inverse dependence of the polarisability on the Madelung potential. To justify this assumption we note that the free O^{2-} ion is an unbound species with the second negative charge being bound only by the Madelung potential. A simplification of the perturbation treatment of polarisability gives, for a single electron:

$$\alpha = 2e^2\langle r^2 \rangle / 3\Delta, \quad (6)$$

with $\langle r^2 \rangle$ the mean square radius of the electronic orbital and Δ a mean excitation energy. Hence if the major contribution to Δ comes from the Madelung energy α will be inversely proportional to this energy.

Our reason for using this crude approximation is that it enables us to apply the shell model in a systematic way to oxides. We take a reference structure in which the oxygen polarisability is α_0 and the corresponding Madelung potential V_0 . Thus α' and V' are the corresponding quantities in a second isostructural crystal,

$$\alpha' = \alpha_0 V_0 / V'. \quad (7)$$

In contrast, we consider the cation polarisability to be less strongly influenced by crystal environment. Mahan has calculated ionic polarisabilities for alkali, halide and chalcogenide ions in crystals with the NaCl structure, and has found that the cation polarisabilities are not significantly affected by their environment. Hence the cation shell parameters will be considered to be transferable between different crystals.

2.2. Empirical fitting procedures

As noted in the Introduction, a major problem in deriving such potentials for oxide materials is the lack of experimental data. This problem may be reduced by using the following assumptions made by Catlow (1977) and Sangster and Stoneham (1980).

(i) The $O^{2-}-O^{2-}$ interaction is taken to be the same for all crystals and the potential derived by Catlow (1977) is used. At equilibrium oxygen–oxygen separations this interaction is very small.

(ii) Cation–cation interactions are assumed to be purely coulombic. Since cations are generally smaller than the oxygen ion and the $O^{2-}-O^{2-}$ interaction already very small at equilibrium lattice spacings this assumption seems to be reasonable.

(iii) The cation–anion interaction is considered to be of the Born–Mayer form.

$$V_{+-} = A \exp(-r/\rho),$$

i.e. the attractive r^{-6} term is ignored. The small contribution of such terms to the short-range potential at the lattice interatomic spacings will be incorporated by small modifications of the Born–Mayer parameters.

For binary oxides the above assumptions (i)–(iii) reduce the problem to the derivation of six parameters, specifying the cation–anion short-range interaction and shell changes and spring constants of the cation and anion. Even so for many oxides there are fewer than six independent experimental observables available. In these cases further assumptions as to the nature of these potentials must be made. In particular it is necessary to consider whole classes of oxides (e.g. the rocksalt structured transition-metal oxides) for which certain parameters may be held in common.

We describe therefore three methods of deriving potential parameters. The first two concern only short-range potentials, and use structural information to fix variable parameters. In the third method, which only applies to crystals for which extensive crystal data are available, both short-range and polarisability parameters are derived for individual crystals in a systematic way. In certain cases, the results obtained by the third method allow us to test the assumptions made in deriving potentials in the first two sections. The three methods are now discussed in detail.

(a) An extrapolation procedure is used for those oxides for which little experimental data is available. We reason that for oxides that are structurally and chemically similar the values of the hardness parameter, ρ , in the Born–Mayer potential will be equal. Thus a constant ρ value is used for the first transition series cation–anion interaction. The A parameters may then be fitted to the lattice parameter, via the equilibrium condition; the resulting values are given in table 1 and their variation across the series is illustrated in figure 1. The table also includes parameters for a number of second and third transition series oxides for which a constant value of ρ is also used; a third constant value is used for the oxides of the lanthanide and actinide metals for which parameters are given in

Table 1. Potential parameters derived using method (a).[†]

Cation	Charge	A (eV)	ρ (Å)
Ca	2	1227.7	0.3372
Sc	2	838.6	0.3372
Ti	2	633.3	0.3372
V	2	557.8	0.3372
Cr	2	619.8	0.3372
Mn	2	832.7	0.3372
Fe	2	725.7	0.3372
Co	2	684.9	0.3372
Ni	2	641.2	0.3372
Zn	2	700.3	0.3372
Zr	4	1453.8	0.3500
Cd	2	868.3	0.3500
Hf	4	1454.6	0.3500
Ce	4	1017.4	0.3949
Eu	2	665.2	0.3949
Tb	4	905.3	0.3949
Th	4	1144.6	0.3949
U	4	1055.0	0.3949

[†] Note that all short-range potentials are truncated (i.e. set to zero) for interatomic spacings greater than 6 Å.

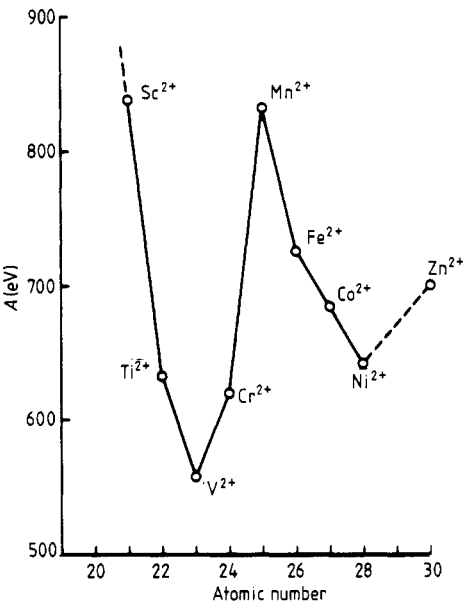


Figure 1. Variation in A (eV) with atomic number for a series of transition metals.

table 1. We note that the three different values of ρ were obtained from the detailed fitting discussed in section (c) below of crystal properties of CaO for the first transition series oxides of SrO for the second and third series oxides and UO_2 for the lanthanide and actinide oxides.

(b) Our second approach exploits the fact that for lower-symmetry crystals the structural data itself contains considerable information; that is, unlike the case for cubic oxides, the equilibrium conditions when applied to unit cell dimensions and atomic coordinates allows more than one parameter to be fixed. Table 2 summarises the parameters for A and ρ obtained in this way for a number of oxides.

(c) For those oxides for which elastic constants, dielectric constants, cohesive energy and structure have been determined experimentally both short-range and polarisability parameters can be obtained. This approach has been used in many previous studies to

Table 2. Potential parameters derived using method (b).

Cation	Charge	A (eV)	ρ (Å)
Sc	3	1299.4	0.3312
Mn	3	1257.9	0.3214
Y	3	1345.1	0.3491
La	3	1439.7	0.3651
Nd	3	1379.9	0.3601
Eu	3	1358.0	0.3556
Gd	3	1336.8	0.3551
Ho	3	1350.2	0.3487
Yb	3	1309.6	0.3462
Lu	3	1347.1	0.3430
Pu	3	1376.2	0.3593

model a particular oxide but here we attempt to derive parameters for several oxides in a systematic and consistent way.

First we note that the dielectric constants are strongly dependent upon the shell parameters, although ϵ_0 is also influenced by the nature of the short-range interactions. Hence, cation-anion interaction parameters for a particular oxide will change somewhat according to the way in which shell parameters are assigned. Two methods of obtaining these shell parameters were used.

In method (i), the magnesium is considered unpolarisable and oxygen shell parameters found by fitting to MgO crystal properties. Using equation (7), the oxygen polarisability is calculated for other crystal structures. By assuming that the cation polarisability values determined for alkaline earth halides are transferable, the potential parameters for CaO, SrO and BaO listed in table 3 were obtained; oxygen shell parameters were determined directly for MgO, CaO, SrO and BaO within the constraints imposed by the polarisability calculated by equation (7). For the other oxides we made use of the fact that the results for the four alkaline-earth oxides show a smooth variation of Y with α for the oxygen ion. This allowed values of Y for each crystal to be interpolated; k is then fixed from the polarisability using equation (5).

In method (ii), the Pauling value of 0.1 \AA^3 is used for $\alpha(\text{Mg}^{2+})$. An approach similar to that of Sangster and Stoneham (1980) is then adopted. Since the right-hand side of equation (2) is determined from experimental data, we can now assign a value to the anion polarisability in MgO. Anion polarisability values in other oxides can then be calculated from equation (7). In this case a fixed value of the oxygen shell charge can be

Table 3. Shell model parameters obtained using method (c)(i). Values for A and ρ refer to cation-oxygen interactions. Values of A in parentheses are appropriate for cations in a tetrahedral anion environment. Structural data are from Wyckoff (1968).

Cation	$A(\text{eV})$	$\rho(\text{\AA})$	Y_-/e	$k_-(\text{eV \AA}^{-2})$	Y_-/e	$k_-(\text{eV \AA}^{-2})$
(i) divalent cations						
Mg	821.6 [710.5]	0.3242	2.0	99999	-2.00	15.74
Ca	1228.9	0.3372	1.26	34.00	-2.82	27.45
Sr	1400.0	0.3500	1.33	21.53	-3.51	39.56
Ba	931.7	0.3949	1.46	14.78	-4.84	70.39
Mn	715.8	0.3464	3.00	81.20	-2.30	19.73
Fe	694.1 [599.4]	0.3399	2.00	10.92	-2.15	17.75
Co	696.3 [600.9]	0.3362	2.00	10.74	-2.06	16.52
Ni	683.5 [593.9]	0.3332	2.00	8.77	-2.00	15.78
Zn	499.6	0.3595	2.05	10.28	-2.00	15.52
(ii) trivalent cations						
Al	1114.9 [1012.6]	0.3118	3.00	99999	-2.21	27.29
Ti	1715.7	0.3069	1.23	43.97	-2.21	27.29
V	1790.2	0.3061	1.34	36.27	-2.21	27.29
Cr	1734.1 [1526.4]	0.3010	0.97	67.00	-2.21	27.29
Fe	1102.4 [876.6]	0.3299	4.97	304.7	-2.21	27.29
(iii) tetravalent cations						
Ge	1035.5	0.3464	4.88	317.2	-2.09	61.5
Sn	938.7	0.3813	3.99	191.5	-3.00	117.8
Ti	754.2	0.3879	2.89	37.3	-2.53	86.4
Ce	1013.6	0.3949	5.85	116.0	-2.67	51.0
U	1055.5	0.3949	6.44	129.0	-2.70	51.6
Th	1147.7	0.3949	7.28	193.1	-2.40	39.0

Table 4. Potential parameters derived using methods (c) (ii).
(i) Cation–anion short-range potential parameters

Cation	Charge	A (eV)	ρ (Å)
Mg	2	1428.5	0.2945
Ca	2	1090.4	0.3437
Sr	2	959.1	0.3721
Ba	2	905.7	0.3976
Mn	2	1007.4	0.3262
Fe	2	1207.6	0.3084
Co	2	1491.7	0.2951
Ni	2	1582.5	0.2882
Al	3	1474.4	0.3006
U	4	1014.3	0.3976

(ii) Shell parameters and ion polarisabilities

Oxide	$\alpha_-(\text{\AA}^3)$	$\alpha_-(\text{\AA}^3)$	Y_-/e	$k_-(\text{eV \AA}^{-2})$
MgO	0.094	2.366	1.585	361.6
CaO	1.284	2.702	3.135	110.2
SrO	2.122	2.899	3.251	71.7
BaO	2.656	3.102	9.203	459.2
MnO	1.773	2.496	3.420	95.0
FeO	2.056	2.421	2.997	62.9
CoO	1.599	2.396	3.503	110.5
NiO	1.718	2.341	3.344	93.7
Al ₂ O ₃	0.052	2.132	1.458	1732
UO ₂	3.759	2.618	5.350	109.7

$\alpha(\text{Mg}^{2-})$ taken from Pauling (1927).

Anion shell charge is taken to be -3.00 (Havinga 1967). Spring constant determined using equation (4.10) and the Madelung potentials determined by Van Gool and Piken (1969).

used following Havinga (1967). The resulting cation polarisability values are given in table 4 together with the Born–Mayer parameters.

2.3. Modelling of changes in cation coordination number

The basic approach adopted follows from the work of Goldschmidt who derived a set of empirical ionic radii from observed interatomic separations. For a cation in an octahedral environment he was able to assign a constant radius, r_{oct} . However it was found that the cation–anion distance does vary slightly with the number of anion neighbours surrounding the cation. From this change of radius with coordination number a ‘correction factor’ is assigned which is the ratio of interatomic distance to the sum of standard radii. For a change from octahedral to tetrahedral coordination the correction factor is 0.94, i.e. $r_{\text{tet}} = 0.94 r_{\text{oct}}$, where d is the interatomic separation.

Using the Huggins–Mayer relationship

$$A = b \exp(d/\rho) \quad (8)$$

we can now modify the short-range cation–anion potential to reflect the change in cation

coordination. Thus

$$A_{\text{tet}} = A_{\text{oct}} \exp(-\Delta r/\rho) \tag{9}$$

where

$$\Delta r = d_{\text{oct}} - d_{\text{tet}} = (0.06)r_{\text{oct}} \tag{10}$$

since the radius of the anion is taken to be constant. Modified potential parameters are given in table 3.

3. Discussion

3.1. Reliability of potentials

The calculation of properties that are not included in the fitting procedure used to derive the potentials provides a useful test of the reliability of the potentials. Table 5 compares the experimental and calculated cohesive energies and elastic constants of a series of oxides using potentials in table 1 derived by procedure (a) described above. The overall agreement is as good as can be expected for rocksalt structured oxides, for which the Cauchy relation ($c_{12} = c_{44}$) applies since central force potentials are used. The general success of the models is satisfactory in view of the derivation of the potentials using an extrapolation procedure.

A more stringent test of our potentials is the calculation of phonon dispersion relations in the principal symmetry directions. In particular, a comparison of calculated and experimental results for the longitudinal optic branches provides a method for checking the extent to which our assumptions are reasonable. Table 6 lists values for

Table 5. Comparison of calculated and experimental cohesive energies (eV) and elastic constants (10^{11} dyn cm⁻²). Potentials were derived using the extrapolative procedure described in § 2.2(a).

Oxide	Calculated		Experimental			Calc. E_{LAT}	Expt. E_{LAT}	
	c_{11}	$c_{12}(=c_{44})$	c_{11}	c_{12}	c_{44}			
(a) NaCl structure								
CaO	22.35	9.87	22.4	6.0	8.1	-36.1	-36.2	
ScO	24.89	13.78	—	—	—	-38.5	-38.9	
TiO	26.59	18.30	—	—	—	-40.6	-40.8	
VO	27.23	21.08	—	—	—	-41.6	-41.1	
CrO	26.86	18.78	—	—	—	-40.8	-41.8	
MnO	24.83	13.87	22.4	11.4	7.8	-38.5	-39.5	
FeO	25.74	15.81	35.9	15.6	5.6	-39.6	-40.7	
CoO	25.94	16.78	25.6	14.4	8.4	-40.0	-41.4	
NiO	26.31	17.98	27.0	12.5	10.5	-40.5	-42.3	
ZnO	25.77	16.40	—	—	—	-39.8	-42.2	
CdO	20.71	11.06	—	—	—	-36.6	—	
EuO	13.08	7.86	—	—	—	-33.2	—	
(b) fluorite structure								
UO ₂	45.1	9.8	6.4	39.6	12.1	6.4	-102.0	-106.8
ThO ₂	42.2	9.9	7.2	36.7	10.6	7.97	-99.9	-104.7
CeO ₂	46.8	10.1	6.4	—	—	—	-102.7	-103.9

Table 6. Experimental and calculated LO frequencies (10^{12} Hz) for (a) MgO and (b) MnO. Experimental values taken from Sangster *et al* (1969) and Haywood and Collins (1969, 1971). Potentials A and B were derived by method (c)(i); potentials E and F using method (c)(ii). Potentials C and D derived by Sangster and Stoneham (1980).

(a) MgO

	q	Experiment	Potential A	Potential C	Potential E
(q00)	0.40	19.82	17.10	19.69	19.78
	0.60	18.07	17.06	17.84	17.91
	0.80	16.78	16.84	16.17	16.40
	1.00	16.61	16.70	15.70	16.05
(qq0)	1.00	13.29	10.80	13.47	13.67
	0.80	14.30	12.34	14.26	14.36
	0.60	16.16	16.04	16.68	16.64
	0.40	19.05	17.40	19.72	19.67
	0.20	20.87	17.10	21.12	21.20
(qqq)	0.10	21.73	17.08	21.43	21.55
	0.20	20.72	17.45	21.26	21.27
	0.30	19.87	18.21	20.95	20.77
	0.40	18.40	19.18	20.49	20.00

(b) MnO

	q	Experiment	Potential B	Potential D	Potential F
(q00)	0.00	14.51	13.62	16.44	15.96
	0.20	13.82	13.63	16.15	15.72
	0.80	8.21	13.17	10.09	10.21
	1.00	8.80	12.70	10.23	10.39
(qq0)	0.20	12.21	13.64	12.62	13.23
(qqq)	0.30	—	13.74	16.27	15.81
	0.35	13.06	—	—	—
	0.40	—	13.76	16.19	15.74

MgO ('best fit') and MnO ('worst fit'). Three types of potential were used. Those in the first column were derived without constraining $\alpha(\text{O}^{2-})$ via equation (2). Comparison with the values obtained using the potentials of Sangster and Stoneham (1980) suggest that a substantial improvement results if equation (2) is used to ensure that the value of $\alpha(\text{O}^{2-})$ is physically reasonable. A further improvement is found when the oxygen polarisability is allowed to vary in accordance with equation (2). Hence with potential E, good agreement with experiment is found. The poorest agreement occurred for MnO. This could to some extent be anticipated since attempts to use the shell model to explain fully neutron scattering results for this crystal have to date proved unsuccessful (Haywood and Collins 1969, 1971). However, it would appear that in general our potentials provide a reasonable description of the statics and dynamics of these rocksalt structured oxides.

We now consider the extent to which our potentials succeed in calculating properties other than those of the perfect lattice. An interesting test is provided by the calculation of activation energies of diffusion for cations in NiO, using the CASCADE defect simulation code (Leslie 1983). This provides a test both of the transferability of our potentials and of the extent to which they are valid for interatomic separations which differ considerably

from those in the perfect lattice. In table 7, these energies are compared with those determined experimentally by Peterson (1984) from tracer diffusion studies. It can be seen that the agreement is generally satisfactory with the largest difference between experimental and calculated energies occurring for self-diffusion. In all cases, the calculated values are slightly lower than those determined experimentally. Since our potential model does not include any explicit treatment of ligand field effects, the small discrepancies are probably attributable to these terms. The results in table 7 thus provide further support for the adequacy of our potential models.

Table 7. Experimental and calculated diffusion activation energies (in eV) for cation diffusion in NiO.

Cation	Calculated	Experimental†
Ni ²⁺	2.3	2.6
Co ²⁺	2.2	2.3
Cr ³⁺	2.9	3.0

† These values will include a contribution from formation energies whose size is uncertain. Such terms should not greatly alter the relative energies of different impurities.

A further test of the reliability of the potentials concerns the modelling of the surface structure, which for MgO has been shown by Rieder (1982) to be rumpled, with cations moving inwards and anions outwards by 0.18 ± 0.02 Å. The structure calculated using the potential for MgO given in table 8 is shown in figure 2. The calculations were performed using the SURFIS simulation code developed by Mackrodt and Stewart (1979). The core displacements in the rumpled surface are calculated to be 0.13 Å inwards for cations and 0.10 Å outwards for the anions. Clearly the correct general magnitude and direction of rumpling is given, although the calculated values are significantly lower than the experimental ones. The discrepancies may be due to changes in the oxygen polarisability in the surface region, which are to be expected in view of the dependence of this parameter on its crystal environment as discussed earlier in this paper.

Finally, we consider the performance of our potential parameters in the modelling of ternary oxides, in particular those with the spinel and perovskite structures. Table 8 gives calculated elastic constants for four spinel structured oxides which have been calculated using the potentials reported in table 3 with short-range parameters adapted for the appropriate coordination number. The results are generally satisfactory, and greatly better than those obtained with models which ignore the dependence of the potential parameters on coordination number.

Table 8. Experimental and calculated elastic constants (10^{11} dyne cm⁻²) for a range of spinel structured oxides.

	Experiment			Calculated (coordinate model)		
	C ₁₁	C ₁₂	C ₄₄	C ₁₁	C ₁₂	C ₄₄
MgAl ₂ O ₄	28.2	15.4	15.4	35.7 (34.4)	18.1 (16.3)	16.7 (15.6)
FeAl ₂ O ₄	26.6	18.2	18.2	35.1 (33.7)	17.9 (16.1)	16.5 (15.3)
ZnCr ₂ O ₄	25.2	14.0	14.0	36.7 (36.7)	16.6 (16.6)	14.1 (14.1)
ZnFe ₂ O ₄	26.5	15.7	15.7	32.2 (32.2)	14.4 (14.4)	13.1 (13.1)

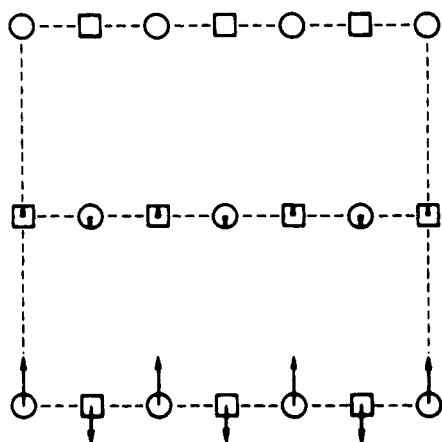


Figure 2. Calculated surface structure of MgO using an empirical potential (table 4). Cations are displaced inwards by 0.13 Å and anions outwards by 0.10 Å.

Furthermore, in a separate study (Cormack *et al* 1984), we show that our model enables the observed 'normal' and 'inverse' cation distributions in a range of spinel oxides to be satisfactorily explained.

Additional evidence for the success in modelling ternary oxides is provided by calculations of the energetics of substitution of a dopant within the perovskite structured BaTiO_3 . Thus it is known that Mn^{3+} substitutes at a Ti site in BaTiO_3 . Table 9 shows the calculated energies of substitution at cation sites in the perovskite structure. We note that empirical potentials predict the correct site of substitution whereas potentials derived using electron gas procedures (see below) predict precisely the opposite results, i.e. that Mn^{3+} will substitute at a barium site.

Table 9. Substitutional energies for the doping of BaTiO_3 with Mn_2O_3 . The empirical potential model suggests titanium site substitution, in accordance with experiment.

Potential type	Energies of substitution (eV)		
	Barium site	Titanium site	Both sites
Empirical	9.52	4.79	5.57
Electron gas	-2.34	6.59	1.28

3.2. Consistency of potentials

To what extent are the parameters reported in tables 1–3 consistent; and how far do our results support the use of simple extrapolation procedures for obtaining potential parameters? The differences between the parameters in tables 3 and 4 are small, reflecting the small differences in the assumptions as to the treatment of polarisability. However, where it is possible to compare the results in table 1 in which the potential parameters for the repulsive interactions were obtained by extrapolation procedures with those in tables 3 and 4 for which detailed empirical fitting was carried out, the agreement is encouraging. In particular the results support the assumption of an approximate constant

value for the hardness factor, ρ , for groups of oxides which was the basis of the extrapolation method. The use of such methods is encouraged by the results.

A further way of checking the general consistency of our results is to examine the extent to which they correspond to known trends in the periodic table. It is therefore satisfactory to note that figure 1 reveals the 'double-minimum' that characterises many trends in the properties of transition metal ions (Orgel 1961). And in general, the trends in our potential parameters are consistent with the known variations in the properties of metal ions.

3.3. Comparison with 'non-empirical' potentials

Considerable effort has been devoted to the derivation of parameters for short-range repulsive potentials using electron-gas procedures based on the methods developed originally by Wedepohl (1967) and Gordon and Kim (1972). Thus Mackrodt and Stewart (1977, 1979) derived potentials by these procedures for alkali halides and alkaline-earth oxides. For many crystals it is found that the potentials derived by empirical and electron-gas methods are similar (see e.g. Catlow *et al* (1982) for a critical discussion). A comparison of values for the alkaline earth oxides is given in table 10.

Table 10. Comparison of empirical and electron gas potential parameters for the metal-oxygen short-range interactions.

	Empirical		Electron gas	
	$A(\text{eV})$	$\rho(\text{\AA})$	$A(\text{eV})$	$\rho(\text{\AA})$
I				
$\text{Mg}^{2+}-\text{O}^{2-}$	1428.5	0.2945	740.7	0.3477
$\text{Ca}^{2+}-\text{O}^{2-}$	1090.4	0.3437	1112.9	0.3541
$\text{Sr}^{2+}-\text{O}^{2-}$	959.1	0.3721	1299.3	0.3635
$\text{Ba}^{2+}-\text{O}^{2-}$	905.7	0.3976	1441.9	0.3723
II				
$\text{Mn}^{2+}-\text{O}^{2-}$	1007.4	0.3262	1088.3	0.3589
$\text{Fe}^{2+}-\text{O}^{2-}$	1207.6	0.3084	1112.7	0.3576
$\text{Co}^{2+}-\text{O}^{2-}$	1491.7	0.2951	1133.4	0.3566
$\text{Ni}^{2+}-\text{O}^{2-}$	1582.5	0.2882	1149.4	0.3557

In our studies of ternary and doped oxides we have, however, found that the empirically derived potentials discussed in this paper perform better than non-empirical methods. Indeed, as shown in the previous section, the latter potentials can yield qualitatively incorrect predictions for the sites occupied by Mn^{3+} in BaTiO_3 . And we conclude following Catlow and Stoneham (1983) that empirical potentials may have an extra component of flexibility over directly calculated ones, since deficiencies in the potential model may, at least in part, be compensated for in the fitting procedure.

4. Summary and conclusions

The work described in this paper has shown that it is possible to derive potential parameters for a wide range of binary oxides which reproduce observed crystal proper-

ties, and which reflect known trends in the Periodic Table. An important feature of our approach has been the inclusion of crystal dependence of the oxygen polarisability. In addition we have found that it is possible to develop extrapolation procedures to derive potential parameters and that the parameters may be used to construct potential models for ternary oxides provided we take account of the effect of coordination number of the short-range potential. The use of these parameters in studying perfect lattice and defect properties of oxides will be amplified in future publications.

Acknowledgments

We would like to thank SERC and STC Components Ltd for supporting the work. We are grateful to Dr W C Mackrodt and Dr E A Colbourn for their collaboration in the calculation of the surface structure of MgO. We also wish to acknowledge a number of useful discussions with Dr A M Stoneham.

References

- Catlow C R A 1977 *Proc. R. Soc. A* **333** 533
Catlow C R A, Corish J, Diller K M, Jacobs P W M and Norgett M J 1979 *J. Phys. C: Solid State Phys.* **12** 451
Catlow C R A, Dixon M and Mackrodt W C 1982 in *Computer Simulation of Solids* ed. C R A Catlow and W C Mackrodt *Lecture Notes in Physics* vol 166 (Berlin: Springer) pp 3–21
Catlow C R A and Mackrodt W C 1982 in *Computer Simulation of Solids* ed. C R A Catlow and W C Mackrodt *Lecture Notes in Physics* vol 166 (Berlin: Springer) pp 130–61
Catlow C R A and Stoneham A M 1983 *J. Phys. C: Solid State Phys.* **16** 4321
Cormack A, Lewis G V and Parker S C 1984 to be published
Dick B G and Overhauser A W 1958 *Phys. Rev.* **112** 90
Gordon R M and Kim Y S 1972 *J. Chem. Phys.* **56** 3122
Havinga E E 1967 *J. Phys. Chem. Solids* **28** 55
Haywood B G G and Collins M F 1969 *J. Phys. C: Solid State Phys.* **2** 46
—— 1971 *J. Phys. C: Solid State Phys.* **4** 1299
Leslie M 1983 *Solid State Ionics* **8** 243
Mackrodt W C 1984 *Solid State Ionics* in press
Mackrodt W C and Stewart R F 1977 *J. Phys. C: Solid State Phys.* **10** 1431
—— 1979 *J. Phys. C: Solid State Phys.* **12** 431
Mahan G D 1980 *Solid State Ionics* **1** 29
Orgel L E 1961 *An Introduction to Transition Metal Chemistry: Ligand Field Theory* (London: Methuen)
Pauling L 1927 *Proc. R. Soc. A* **114** 181
Peterson N L 1984 *J. Phys. Chem. Solids* in press
Rieder K H 1982 *Surf. Sci.* **118** 57
Sangster M J L, Peckham G and Saunders G H 1969 *J. Phys. C: Solid State Phys.* **3** 1026
Sangster M J L and Stoneham A M 1980 *Phil. Mag.* **43** 597
Van Gool W and Piken A G 1969 *J. Mater. Sci.* **4** 95
Wedepohl P J 1967 *Proc. Phys. Soc.* **92** 79
Wyckoff R W G 1968 *Crystal Structures* vol. 1 and 2 (New York: Interscience)